INTERNATIONAL JOURNAL OF PRECISION ENGINEERING AND MANUFACTURING Vol. 19, No. 9, pp. 1305-1315 SEPTEMBER 2018 / 1305

REGULAR PAPER

DOI: 10.1007/s12541-018-0154-4
ISSN 2234-7593 (Print) / 2005-4602 (Online)

Terrain Classification for Mobile Robots on the Basis of Support Vector Data Description

Hyunsuk Lee[1] **and Woojin Chung**[1,#]

1 Department of Mechanical Engineering, Korea University, 145, Anam-ro, Seongbuk-gu, Seoul, 02841, Republic of Korea
Corresponding Author / E-mail: smartrobot@korea.ac.kr, TEL: +82-2-3290-3375
ORCID: 0000-0001-8833-1864

KEYWORDS: Mobile robot, Traversability analysis, Classification, Obstacle detection, Mapping

The ability to detect traversable terrains is essential for autonomous mobile robots to guarantee safe navigation. In this paper, we present a method for terrain classification for wheeled mobile robots. Our scope is limited to mobile service robots that are used for surveillance or delivery in semi-structured urban environments. A reliable terrain detection scheme is required for both indoor and outdoor applications anytime. A low-cost Lidar (Light detection and ranging) is adopted for terrain detection. To deal with intrinsic measurement errors and uncertainties of the Lidar, the classification criteria are trained through a supervised learning approach. Training data are obtained from manual driving at target environments. Various decision boundaries resulted from a variety of floor conditions, sensor types and robot platforms. The proposed terrain classification scheme is experimentally tested in success.

Manuscript received: March 31, 2017 / Revised: March 20, 2018 / Accepted: July 11, 2018

1. Introduction

In recent years, autonomous mobile robots have been commercialized in industrial fields.[1-3] Service robots with autonomous navigation capability are used in hospitals[4] and hotels.[5] Mobile robots operate in our daily life, where robots and humans coexist. In a human environment, a typical terrain contains various obstacles such as protruding obstacles, stairs, and holes, as shown in Fig. 1. Failure to avoid terrain obstacles introduces the risk of a robot being stuck and overturned, which may result in damage to the robot as well as bodily injury to the service users. Ensuring robot safety based on the traversability analysis significantly lowers the risk of serious accidents in mobile robot applications. In a structured environment, two-dimensional (2D) laser sensors are sufficient to detect obstacles. Therefore, most of the commercialized robot platforms have used 2D laser sensors for navigation. However, the mobile robot that use a planar 2D laser sensor should equip additional sensors for detecting terrain. Without reliable methods for terrain detection, global navigation by wandering is not allowed when the robot pose is missing.

In this paper, we present a terrain classification method for ensuring navigation safety of mobile service robots, which operates in semi-structured urban environments. Our requirements of considerations for implementing a terrain classification method for mobile service robots are summarized as follows: (1) Navigation in indoor and outdoor urban environments, excluding unstructured rough terrain. (2) Reliable performance regardless of illumination change. (3) Precise detection of hazardous regions. (4) Capability to cope with various terrain types, sensors and robots. (5) Real time, low cost sensor.

Fig. 1 Terrain obstacles in human environments

Significant attention has been devoted to developing vision-based methods of terrain traversability analysis.[6-9] However, vision sensors have not been primarily used in outdoor environments owing to the well-known problem of illumination dependence of detection performance. On the other hand, Lidars (Light detection and ranging) have been widely utilized for terrain classification. The Lidars are

advantageous because they provide accurate range measurements irrespective of changes in the environment in which they operate.

Recently, three-dimensional (3D) Lidars have been increasingly considered for environmental perception of autonomous vehicles.[10] Mobile robots are typically quite small and move at a lower speed than vehicles. Therefore, it is effective to precisely measure the terrain in the vicinity of a robot, rather than in a remote area. Although commercial 3D laser sensors provide a large amount of point clouds, their vertical field of view makes it hard for a robot to measure a nearby terrain. In addition, owing to their exorbitant price, mounting an additional 3D laser sensor is not easy in service applications using mobile robots. A possible solution is to use a 2D laser sensor inclined toward the ground. Recent short range Lidars are commercially available under $300, and the cost is decreasing fast. A terrain can be accurately measured by a tilted 2D laser sensors, which focus on the terrain in the vicinity of a robot. Data processing is also more efficient because the majority of the scanned data correspond to the terrain. Andersen et al. detected traversable regions by using a 2D laser sensor inclined at a fixed angle.[11] C. Ye built an elevation map for the terrain traversability analysis (TTA).[12,13] The elevation map was constructed in the grid representation, in which each grid cell was assigned a traversability index. A similar approach was suggested by Y. Tanaka et al.[14] The weakness of these methods is that they depend on heuristic thresholds for extracting traversable regions from scanned data. The heuristic thresholds should be redefined when operational conditions are changed.

When a terrain is scanned by using a Lidar, the measurements depend on the operational conditions such as robots, sensors, and terrain types. Therefore, obstacle detection based on the geometric relations in the scanned data is difficult in general. It is important to derive classification criteria that could be easily adapted in different operational conditions. Supervised learning has been widely exploited for terrain classification to deal with various operational conditions.[15] For detecting negative obstacles in an off-road environment, a method for terrain classification was proposed by J. Larson and M. Trivedi.[16] They made use of support vector machine (SVM) based classifier, which was learned based on the geometric features of negative obstacles. K. M. Wurm et al. proposed a terrain classification approach for detecting low vegetation in structured outdoor environments by using the SVM and linear discriminant analysis (LDA).[17,18] In these approaches, classifiers were learned based on range, reflectivity, and incidence angle. The learned classifiers could distinguish vegetation from streets with high accuracy. However, their studies are different from our interest in that the classifier did not consider the detection of obstacles. Principal component analysis (PCA) has also been used to learn classifiers for detecting drivable surface from the 3D point clouds.[19-21] The above-mentioned methods require constructing training data sets that contain negatively labeled data as well as positively labeled data. Therefore, operators should amass large amounts of data not only for non-traversable terrains but also for various types of obstacles. These approaches also involve exhausting tasks of hand-labeling the training data set as individual classes.

Detecting hazardous terrains is the same as detecting outliers in terrain data. This problem can be solved using a decision criterion that is learned by the samples from the traversable parts. B. Sugar proposed a method for traversability analysis based on a semi-supervised approach.[22] A. Santamaria-Navarro also suggested a method for terrain classification that exploits Gaussian process.[23] To obtain traversable samples from the target environment, in both works, footprint data of the robot trajectory were collected by manually operating the robot. This approach is advantageous because the training data can be easily obtained without hand-labeling a large number of data set. However, both of the above works are not suitable for the detection approach that uses a 2D laser sensor, because they use terrain features from 3D point clouds, which are measured by using a 3D laser sensor. There is a lack of research on terrain classification that uses only positive labeled data based on a 2D laser sensor.

In this paper, we propose a method for terrain classification using a 2D Lidar with a fixed tilting angle. Our approach is especially suitable for mobile service robots that are used for surveillance, transportation, and entertainment in semi-structured urban environments. The capability of traversing obstacles depends on an individual platform that is used in a specific application. Therefore, we learned the classification criterion for traversable regions on the basis of a supervised learning approach for individual operational conditions.

The contribution of this paper is twofold. The first contribution is a method for the range calibration of laser sensors. The geometry of the terrain surface is distorted due to the intrinsic bias errors of a laser sensor. A geometric relation between a scan point and flat terrain is considered to estimate the errors. Secondly, we propose a method for terrain classification to detect traversable terrains by using a 2D laser sensor. We use the data collected from the footprint area, which is already known as a traversable terrain. All an operator has to do is simply steer the platform through a traversable terrain in a target environment. Because the collected samples are only composed of traversable positive samples, we utilize the support vector data description (SVDD), which is appropriate for detecting negative outlier samples. Our approach allows to deal with a variety of operational conditions, and assures the robustness of terrain classification for individual platforms.

The remainder of this paper is organized as follows. In Section 2, we suggest a method for pre-processing of the range data for bias calibration. A classification scheme based on SVDD is presented in Section 3. In Section 4, we describe several experimental results that include terrain classification in indoor and outdoor environments.

2. Range Data Pre-Processing

The measurement accuracy of a terrain measured by a Lidar depends on sensor types and terrain materials. Adams and Probert suggested that bias errors of laser sensors are relevant to an internal gain amplifier that leads to amplitude-induced range errors.[24] The researchers found that these range errors of laser sensors are affected by the materials, colors, and distance to a target object.[25,26] Based on their empirical data, they built a calibration model that the true distance is given as a linear combination of the mean value of the range measurements and the constant bias. In a similar way, Borges et. al. proposed a method for the bias compensation of Lidar beams.[27] They suggested that the bias error is varying with true distance. The bias of Lidar beams is approximated by a sixth-order polynomial. Although above work achieved improved results in range measurements, they assumed that all beams of a sensor have the same bias. However, biases of Lidar beams differ from each

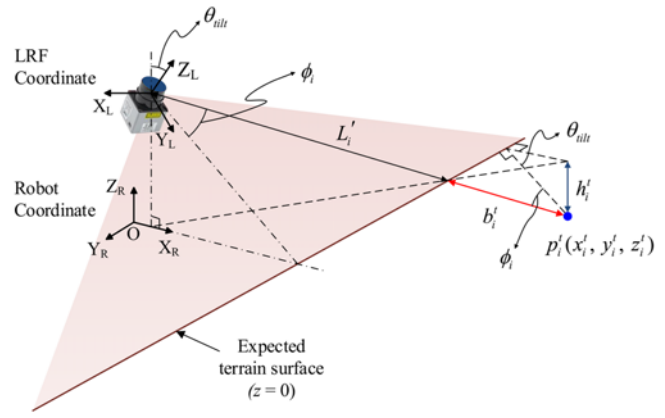

Fig. 2 The configuration of an 2D Lidar and a flat terrain

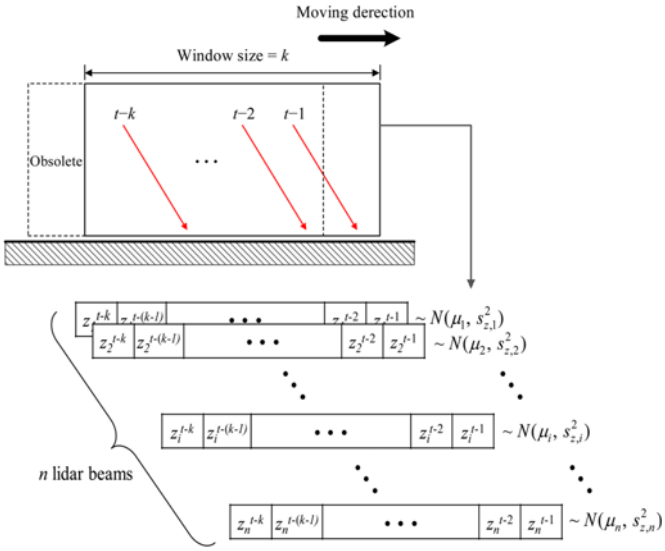

Fig. 3 Rolling window for the feature extraction

other. In our approach, the bias errors of each Lidar beam are estimated by using a geometric relation between scan points and flat terrain.

In this section, we present a method for calibrating the intrinsic bias error. Since the intrinsic bias error is induced by the gain amplifier of the sensor, we assume that the bias error is not related to the movement of the robot. Therefore, our approach estimates the intrinsic bias by calculating height measurement errors of the ground surface when a robot is in a static condition. Fig. 2 presents the configuration of the robot equipped with a tilted 2D Lidar. The height of the terrain surface at each scan point is estimated by the Kalman Filter. If the surface is flat, the height of the expected terrain surface converges to 0. When height measurement z_i^t and noise σ_i of the i-th scan point p_i are given, estimated terrain height h_i^t and its variance v_i^t are calculated as follows.

$$h_i^t = \frac{(\sigma_i)^2 h_i^{t-1} + v_i^{t-1} z_i}{v_i^{t-1} + (\sigma_i)^2} \tag{1}$$

$$v_i^t = \frac{v_i^{t-1}(\sigma_i)^2}{v_i^{t-1} + (\sigma_i)^2} \tag{2}$$

The height of each scan point are estimated by Eq. (1) while the tilted Lidar measures a flat terrain during [0, t]. If we assume that the heights of the flat terrain are zero, estimated height h_i is the measurement error of the i-th scan point. Range bias error b_i of the i-th scanned point can be calculated from h_i by using a geometric relation as shown in Fig. 2. b_i is calculated as

$$b_i = \frac{h_i}{\sin(\theta_{tilt}) \cdot \cos(\phi_i)} \tag{3}$$

where θ_{tilt} is the tilting angle of the Lidar, and ϕ_i is the orientation of the i-th measurement point. Calibrated range $L_i' = L_i + b_i$, which is the linear combination of measured range L_i and bias b_i, is used for calculating the coordinates of each scanned point. After the bias calibration, the scanned points have zero mean with Gaussian noise when the Lidar measures the flat terrain. As a result, the intrinsic sensor errors can be calibrated.

3. Terrain Classification

3.1 Terrain features

For terrain classification, it is important to consider terrain characteristics that can distinguish traversable regions from obstacles. In structured urban environments, a robot moves through a terrain, most of which consists of smooth surface, and the vicinity of the robot is mostly traversable area. In these environment, it is reasonable to regard occasional hazardous regions as outliers of scanned data. Our approach uses previous and horizontal information of scanned data for detecting outliers.

One of the features is a Mahalanobis distance between new height measurement z_i of a current scanned point and previous height measurements. A measurement which has large Mahalanobis distance to previous distribution has a large possibility of a non-traversable point, because the robot previously drives through a safe region. A rolling window with size k is utilized to compute this feature. The previous height measurements during time interval [t-k, t-1] are accumulated in the rolling window, as shown in Fig. 3. For each Lidar beam, the feature is computed as follows.

$$d_i = (z_i - \mu_i)^2 / s_{z,i}^2 \tag{4}$$

μ_i and $s_{z,i}$ are the mean and the standard deviation of the previous height measurements of the i-th scanned point, which are accumulated in the rolling window. By using the information in the rolling window, this feature can indirectly reflect the terrain roughness for a 2D laser sensor that yields a sparse data set in a single scan.

Differences between the terrain surface and measurements are also used to calculate a terrain feature. Because terrains of the urban environments mostly consist of smooth surfaces, there is a strong likelihood that measurements, which have large difference from a terrain surface, are non-traversable region. We detect the floor surface from single scan measurements at time t, and compute differences e_i. This feature is computed from the difference as

$$r_i = (e_i - m_t)^2 / s_{r,t}^2 \tag{5}$$

where m_t and $s_{r,t}$ are the mean and the standard deviation of the

differences for a single scan at time t. This feature yields a normalized deviation of the i-th scan point from the terrain surface.

There are several methods for detecting the terrain surface. The least square method is simply used for surface detection in structured indoor environments, because the entire area is flat. In this work, Gaussian process regression (GPR) is used for terrain detection in order to deal with non-flat terrain surfaces in outdoor environments. Segmentation was performed on single-scan data by using the split-and-merge approach. Thereafter, position (x, y) of the scanned points on the line segment that corresponds to the terrain surface is used as the input vector, and height value z of the scan point are estimated by GPR. A squared exponential function is used as a covariance function.

3.2 Support vector data description (SVDD)

SVDD is one of the methods of supervised learning that deals with one-class classification problem.[28,29] The goal of SVDD is to define a ball-shaped decision boundary that includes normal positive samples in the feature space. For this reason, this method has been used for outlier detection in various fields. Therefore, it allows to define a decision boundary when there are no negatively labeled samples. An optimal boundary is defined by a following equation.

$$\begin{aligned} &\min_{R^2,\,\mathbf{a},\,\xi} \; F(R,\mathbf{a}) = R^2 + C\sum_i \xi_i \\ &\text{s.t.} \quad \|\mathbf{x}_i - \mathbf{a}\|^2 \le R^2 + \xi_i, \qquad \xi_i \ge 0\,, \qquad \forall i \end{aligned} \tag{7}$$

n is the number of training samples $\mathbf{x}$. The decision boundary is a sphere that is centered at $\mathbf{a}$, and its radius is R. Variable ξ_i is a slack variable, which is assigned to outliers that deviate from the decision boundary. Parameter C regulates trade-off between the volume and the outliers. Classification of linearly non-separable data can be performed by applying a kernel function.

3.3 Terrain classification on the basis of SVDD

Detecting obstacles on a terrain is analogous to a problem of detecting outliers. Our approach for terrain classification defines classification criteria based on the features of the traversable terrain. An obvious way to obtain the data on traversable parts is to collect footprint data by steering the robot platform. By using the footprint data, we calculate the terrain features that are described in Section 3.1. However, the obtained data are only composed of positively labeled samples. Therefore, it is important to adopt a learning algorithm to deal with this type of data.

In our approach, we adopt SVDD for classification. In comparison with other supervised learning methods, an important advantage of SVDD is that users do not need to hand-label the training data from traversable regions to obstacles. In this approach, users simply model characteristics of traversable regions, and the classification criteria can be learned from the features of the traversable regions. Therefore, SVDD is appropriate for our problem.

In this work, training data $D = \{(\mathbf{x}_i, y_i) \mid i = 1, 2, \ldots, n\}$ are generated for a traversable terrain. $\mathbf{x}_i$ is a positively labeled data vector that comprises two terrain features $[d_i, r_i]$. y_i is a scalar that corresponds to the class label. Since the training data contain only positively labeled samples that correspond to traversable parts, y_i is 1.

For computational efficiency, we randomly subsampled a large number of training data that we amassed from the footprints. The classification boundary was learned from the subsample. The Gaussian radial basis function (RBF) was used as a kernel function for non-linear classification of the training data. The optimal parameters that resulted in the highest classification accuracy were determined by a fivefold cross-validation.

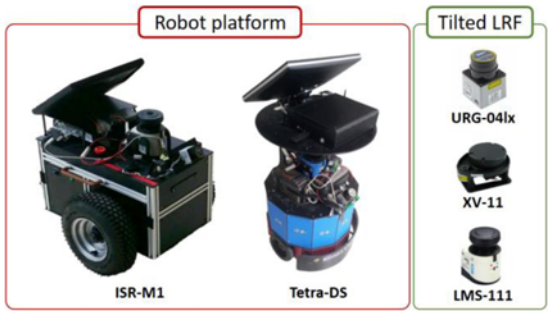

Fig. 4 Mobile robot platform and sensor configuration

Terrain feature data are different under different operational conditions, e.g., for different ground materials, sensor types, and platform-dependent vibration. Therefore, our approach is to collect the training data for various operational conditions, thereby defining different SVDD classification boundaries.

Let $\mathbf{z}_{new} = [d_{new}, r_{new}]$ be an arbitrary vector from a real-time measurement in target environments. The decision function to classify the arbitrary vector is given as follows.[28]

$$\mathbf{F}(\mathbf{z}_{new}) = 1 - 2\sum_i \alpha_i K(\mathbf{z}_{new}, \mathbf{x}_i) + \sum_{i,j} \alpha_i \alpha_j K(\mathbf{x}_i, \mathbf{x}_j) \tag{8}$$

where, α_i is the Lagrange multiplier that is obtained from the training data. The decision function corresponds to a mapping function, which project the feature vector to the trained feature space. The output of the Eq. (8) is given as a scalar, which means the distance from the center of the decision boundary. If the distance is larger than the radius of the boundary, new feature vector $\mathbf{z}_{\text{new}}$ is classified as an obstacle. The traversable points are $R_t = \{\mathbf{z}_{\text{new}} \mid \mathrm{F}(\mathbf{z}_{\text{new}}) \le R^2\}$, and the obstacles are $R_o = \{\mathbf{z}_{\text{new}} \mid \mathrm{F}(\mathbf{z}_{\text{new}}) > R^2\}$ in the classification step.

When a target environment contains two or more ground materials, SVDD boundaries should be separately defined according to the ground materials. The local maps should contain terrain type information, and the SVDD boundaries are trained for each terrain type.

4. Experiment

4.1 Hardware setup

To validate our algorithm, we analyzed the bias errors and terrain features under different operational conditions. We conducted experiments in indoor and outdoor environments with different terrain types. The platforms and the sensors that were used in these experiments are shown in Fig. 4. We used two different platforms for data collection. Tetra-DS was used for indoor environments, and ISR-M1 was used both for indoor and outdoor environments. In order to detect the terrain, Neato XV-11, Hokuyo URG-04lx, and SICK LMS-111 were alternately mounted on a pan-tilt unit. The Xsens MTI IMU was attached for measuring the platforms' attitude.

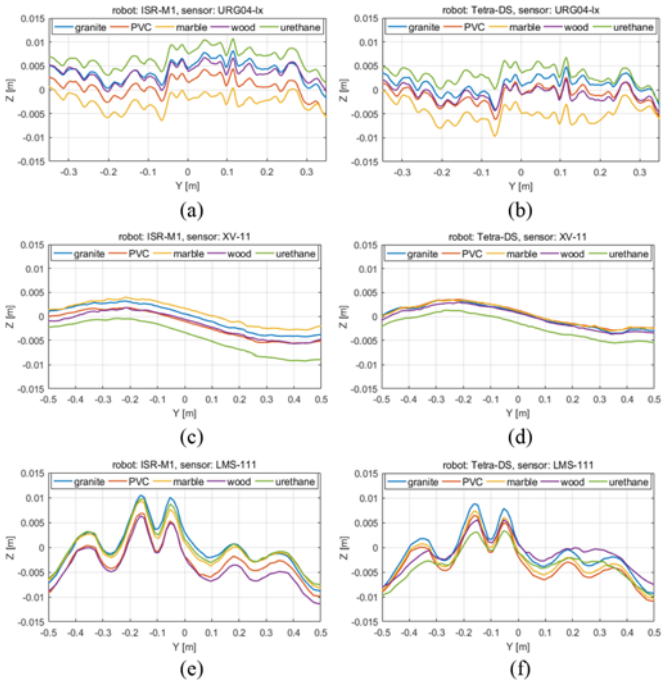

Fig. 5 The means of the height measurements of the flat terrain surface in driving conditions; (a) Robor: ISR-M1, sensor: URG-04lx, (b) Robot: Tetra-DS, sensor: URG-04lx, (c) Robot: ISR-M1, sensor: XV-11, (d) Robot: Tetra-DS, sensor: XV-11, (e) Robot: ISR-M1, sensor: LMS-111, (f) Robot: Tetra-DS, sensor: LMS-111

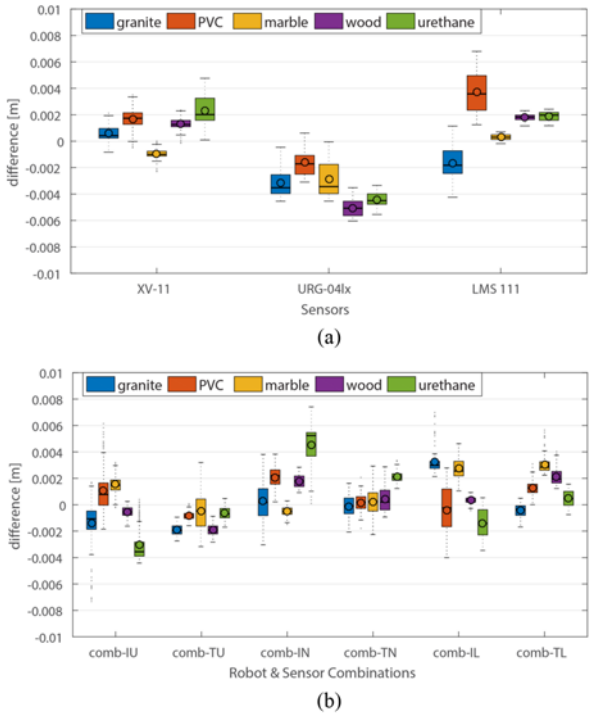

Fig. 6 Difference between the floor height measurements (a) by different robots and (b) in the static and driving conditions: comb-IU (robot: ISR-M1, sensor: URG-04lx), comb-TU (robot: Tetra-DS, sensor: URG-04lx), comb-IN (robot: ISR-M1, sensor: XV-11), comb-TN (robot: Tetra-DS, sensor: XV-11), comb-IL (robot: ISR-M1, sensor: LMS-111), comb-TL (robot: ISR-M1, sensor: LMS-111)

4.2 Lidar bias calibration

In this section, we computed the bias errors of the Lidar by the use of empirical data. The experiments were conducted in structured indoor environments. We measured five different terrain types. The terrain data were obtained using two different platforms and two different Lidars in driving and static conditions.

Fig. 5 shows the height measurements of the flat terrain surface in the driving condition that were represented in the robot's local y-z plane. Although the surface is flat, there are many nonzero mean values of the height measurements. In other words, the geometry of the terrain surfaces was not accurately measured, owing to the bias errors. Moreover, the geometric shapes depend on sensor types, and the mean values of the measurements were different under different terrain types. Consequently, we concluded that terrain types and sensor types affect bias errors.

In order to investigate the effect of the platform type on the measurement accuracy, we calculated differences between height measurements for different platforms equipped with the same sensor. The results are shown in Fig. 6(a). Height measurements by the same sensor mounted on different platforms did not show any significant differences, because the measured peak-to-peak values for all terrains were within 0.005 m. We concluded that the type of a platform does not affect terrain bias errors. We also considered the effect of driving state on bias errors. Fig. 6(b) shows the difference between height measurements in static and driving conditions of a platform. The results are shown for all possible combinations of the sensors and platforms. In Fig. 6(b), mean values are within 0.003 m for all of the considered terrain types, and peak-to-peak values are mostly within 0.005 m. Although the vibrations associated with driving were taken into consideration, the result shows that there is no significant difference between the robot's static and moving conditions. In other words, the driving state of a platform does not affect terrain height measurements. The above experiments indicate that the primary factors underlying range bias errors are sensors and terrain types.

In order to calibrate the bias errors, the proposed method in section 2 was applied in static conditions. The robot in this experiment was Tetra-DS. Two different Lidars were used to scan the terrain. The bias error of each Lidar beam was estimated by Eq. (3). The calibrated range measurements were derived by adding the bias to the range measurement. The coordinates of the scanned points were calculated by the calibrated range. The height measurements of the ground after bias calibration is shown in Fig. 7. Compared with Figs. 5(b), 5(d), and 5(f), these results imply that each scanned point of Lidars can measure the true height of a flat terrain surface ($z = 0$), after applying the proposed bias calibration method.

The advantage of applying the bias calibration method is apparent from a case of detecting small obstacles. We conducted a simple experiment to detect an 1cm obstacle in Fig. 8(a). Measurement points were accumulated and projected to y-z plane of the robot coordinate while a robot navigated toward the obstacle. Figs. 8(b) and 8(c) show the projected scanned points before and after calibration, respectively.

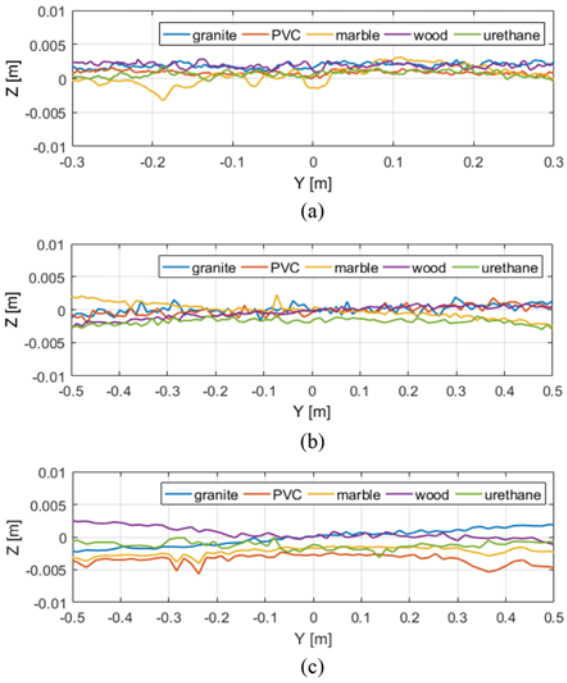

Fig. 7 Height measurements of ground after bias calibration; (a) Robot: Tetra-DS, sensor: URG-04lx, (b) Robot: Tetra-DS, sensor: XV-11, (c) Robot: Tetra-DS, sensor: LMS-111

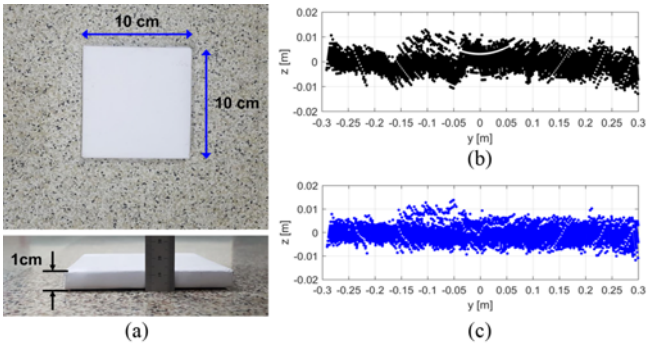

Fig. 8 Raw measurements of an 1-cm-tall obstacle. (a) an obstacle. (b) Before bias calibration. (c) After bias calibration

The obstacle was located within the range of -0.15 cm $\leq y \leq$ -0.05 cm in both graphs. Before the bias calibration, the points of the obstacle were visually indistinguishable from those of the terrain surface, as shown in Fig. 8(b). On the other hand, after applying the proposed method, the scanned points are distributed around the height of zero, which corresponds to the flat terrain, as shown in Fig. 8(c). In addition, the obstacle within the range of -0.15cm $\leq y \leq$ -0.05 cm is visually identifiable by the measurement points in the vicinity of 1cm height. The result implies that there is a strong possibility to detect obstacles as small as 1 cm in height by using the proposed method.

4.3 SVDD training results

To train a classification boundary for traversable region, training data were collected from the traversed region when a mobile robot was manually steered in a target environment. In such a way, the positive labeled data, which corresponds to traversable region, could be collected much easier without hand-labeling. In our approach, SVDD, which can handle only positive-labeled data, was exploited to learn the classification boundaries. In other words, there is no need to accumulate negative-labeled data that cannot be traversed by a robot. For improving the classification accuracy, our approach adopted different classification boundaries when operational conditions were changed. Fig. 9 shows the learned boundaries for training data set for different operational conditions, where different platforms, different sensors, and different terrain types were considered. The distributions of these training data depend on individual operational conditions. In this context, the shapes of the learned SVDD boundaries were different according to different operational conditions. Therefore, we conclude that classification boundaries should be redefined when operational conditions are changed.

4.4 Terrain classification in indoor environment

The experimental environment was a well-structured indoor environment that consists of a flat floor, vertical walls, and stairs. We used the Tetra-DS platform, which was not able to traverse across obstacles taller than 1 cm in height. Therefore, we constructed an experimental environment by placing arbitrary obstacles that were taller than 1 cm. We steered the robot manually through the test scene to encounter all obstacles. For terrain classification, Hokuyo URG-04lx was tilted toward the floor, with a fixed angle of 70°. Because the indoor robot navigates with a low speed, the robot only has to detect obstacles that are in its vicinity. Therefore, we limited the field of view to ±35°. The classified obstacles were mapped onto the local map, according to the localization results. To estimate the robot's pose, we used Monte Carlo-based localization (MCL) with an additional planar 2D Lidar.[30]

From the results in section 4.3, we verified that the classification boundary should be defined according to individual condition changes. The changes in operating condition include terrain types as well as sensors and platforms. In this experiment, the test scene consists of two different floor materials (PVC and granite), which means that two individual operating conditions exist in the environment. Hence, we trained the two SVDD boundaries for each material type, and these boundaries were used to classify the laser scan points. In order to apply the appropriate boundary to the measured points, the information of the floor material was given in the global map.

Fig. 10 shows the terrain classification results of the experimental environment. The blue dotted line represents the robot trajectory that was estimated by the MCL. The traversable area is represented with black dots, and the detected obstacles are marked with red dots. The obstacles below the height of a horizontal 2D laser were detected correctly. Moreover, our algorithm successfully detected the obstacles as small as 1 cm in height, which Tetra-DS was unable to traverse. The braille block near the stairs was 0.5 cm in height. Because this height is within the measurement error of the laser sensors, in the strict sense it cannot be detected. In this experiment, the braille blocks were detected owing to their reflective material (stainless steel) that yielded range measurement errors. With all things considered, our algorithm was able to detect the obstacles taller than 1 cm as well as the negative obstacle (stairs) in the structured indoor environment, which could not be traversed by the robot.

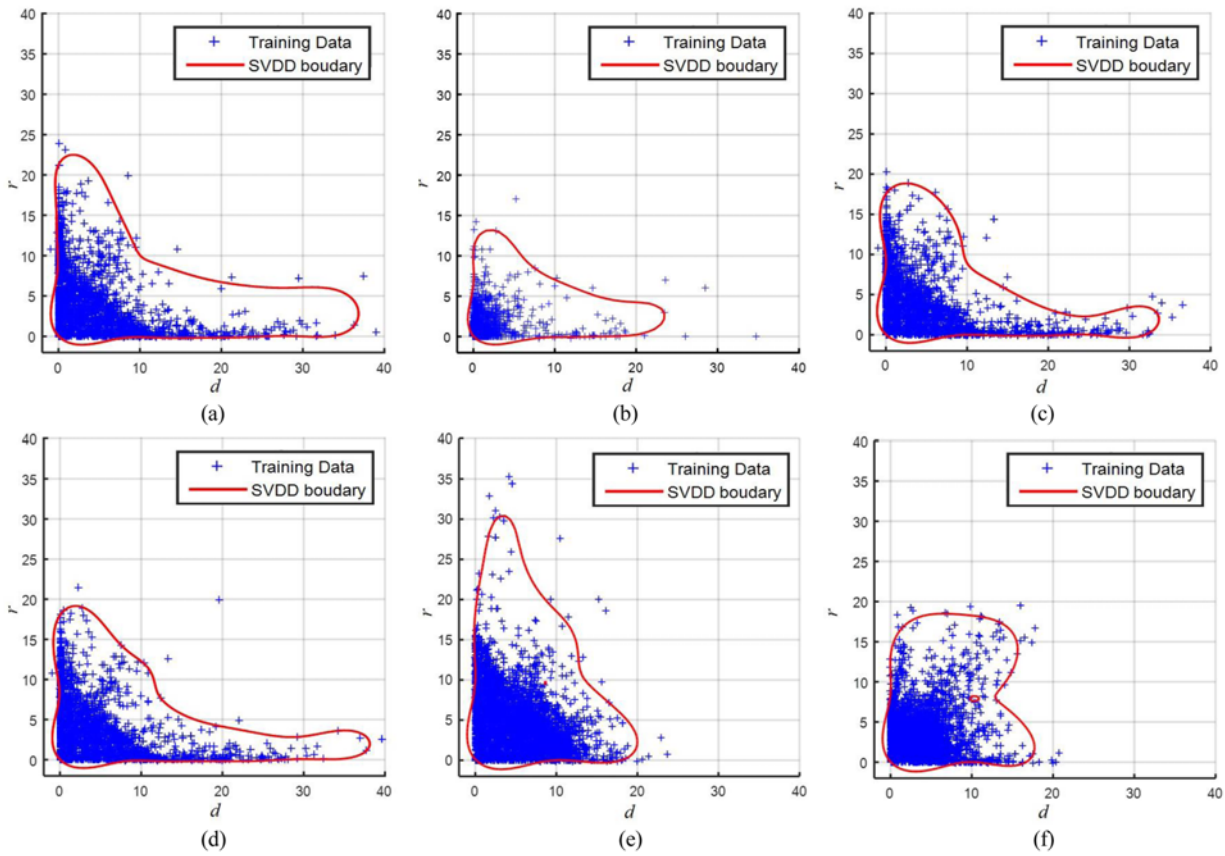

Fig. 9 SVDD boundary and training data, for different operational conditions; (a) Robot: ISR-M1, sensor: URG-04lx, floor material: PVC, (b) Robot: Tetra-DS, sensor: URG-04lx, floor material: PVC, (c) Robot: ISR-M1, sensor: XV-11, floor material: PVC, (d) Robot: ISR-M1, sensor: URG-04lx, floor material: granite, (e) Robot: ISR-M1, sensor: LMS-111, floor material: granite, (f) Robot: ISR-M1, sensor: LMS-111, floor material: cement brick

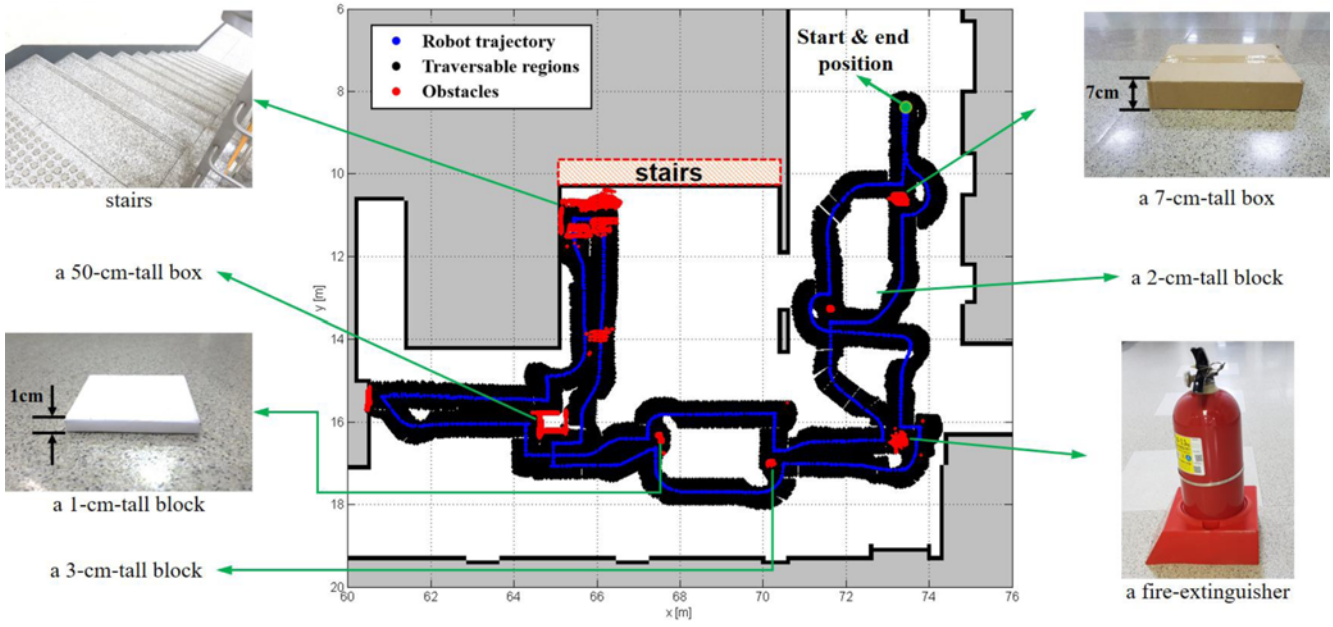

Fig. 10 Terrain classification results for the indoor environment

In order to evaluate the classification results, we marked the misclassified points manually. Table 1 shows the confusion matrix of the classification results. Among 758,632 points in total, 706,263 were traversable and 52,369 corresponded to obstacles. The precision, recall,

Table 1 Confusion matrix for the indoor experiment

		Classification results		Subtotal
		traversable	obstacle	
Actual	traversable	703,666 (99.63%)	2,597 (0.37%)	706,263
	obstacle	95 (0.18%)	52,274 (99.82%)	52,369
Subtotal		703,761	54,871	758,632

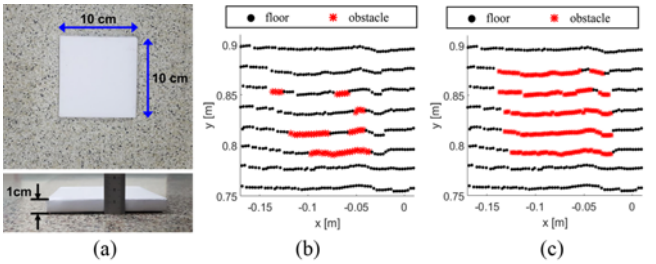

Fig. 11 Detection of a 1-cm-tall obstacle; (a) The obstacle on the surface of PVC material, (b) Detected by inappropriate boundary (SVDD boundary: wood), (c) Detected by appropriate boundary (SVDD boundary: PVC)

and specificity values were 0.9999, 0.9963, and 0.9982 respectively. These results indicate that the obstacles, as well as the traversable regions, were classified with high accuracy.

The effectiveness of our approach can be verified by a comparative result when an inappropriate boundary is used for terrain classification. Fig. 11 presents the classification results for an obstacle, which was conducted by the use of two different boundaries. Fig. 11(a) shows an 1-cm-tall obstacle on the floor of a PVC material. In Fig. 11(b), the obstacle was detected by the classification boundary for wood material, which is inappropriate for this operating condition. The specificity was 0.2895 (55/190 points). Since the result shows a large type I error, the inappropriate boundary could hardly detect the obstacle. Consequently, the robot has a strong possibility to collide with the obstacle. The classification result by the boundary for the PVC material is shown in Fig. 11(c). In this case, specificity was 0.9632 (183/190 points). This result implies that most of the obstacle points could be detected by the use of the appropriate boundary. Therefore, in order to classify the terrain with high accuracy, an SVDD boundary should be designated properly with regard to a given operational condition.

Without bias calibration, obstacles taller than 3 cm were only visible in the cumulated data. However, with our approach, the geometry of terrains could be measured precisely, and the obstacles taller than 1 cm were detected with high resolution by applying an appropriate SVDD boundary.

4.5 Terrain classification in outdoor environment

Using the same approach, we conducted an experiment in an outdoor environment. In this experiment, we validated the effectiveness of our algorithm by using different sensors and different robots. We steered an ISR-M1 platform across the campus environment. SICK LMS-111 was tilted to 55° toward the ground for the terrain detection. For computational efficiency, we used the terrain data for classification within the field of view of 180° and the range of 8 m. An additional GPS system was attached for estimating the robot pose in the campus environment. The robot pose was estimated by GPS-IMU based EKF localization. Travel distance of the robot was about 556 m. The environment consists of five ground material types (granite, wood, cement, asphalt, and vegetation). It means there were five different operating condition in this environment. The experimental environment was comprised of protruding obstacles such as boundary stones of flower gardens, trees, benches, and walls. Negative obstacles, such as stairs, ponds, drains, and curbs also exist.

In the experiment that was conducted in the structured indoor environment, the indoor robot is not able to move over obstacles as small as 1 cm in height. Accordingly, when the proposed bias calibration was applied to the terrain classification, the minimum height of the obstacle that could be detected by the proposed method was 1 cm. On the other hand, As ISR-M1 is capable of traversing obstacles up to 4 cm, it is sufficient to detect obstacles of 4 cm or more in height. Therefore, the bias calibration method was not used in this experiment. For each terrain type, the classification boundaries were trained using the footprint data by the application of the same approach in section 4.4. Because the local map of the campus scene was not available, we divided the area that consists of different materials in accordance with the GPS coordinates. Classification was conducted using the SVDD boundary, which corresponded to the current robot pose.

Fig. 12 shows the classification results, which are mapped according to the EKF localization results. Traversable points are represented in green dots, and obstacles, which are non-traversable for ISM-M1, are shown as gray dots. Several hazardous regions are represented by magnified views. The proposed terrain classification shows accurate and reliable performances in various environmental conditions. To evaluate our algorithm, we hand-labeled the scan points as positive and negative ground truth, considering that ISR-M1 was not able to traverse over obstacles taller than 4 cm. The ground truth was used to evaluate our algorithm. The precision and recall values were 0.9903 and 0.9977, respectively. The traversable points were classified as traversable points with high accuracy. In terrain classification, one of the most important factors is specificity that implies the classification accuracy of the obstacle data. In this experiment, the specificity factor was 0.9378, which was relatively low compared with the result of the indoor experiment. However, considering that the measurement accuracy of the laser sensor is 3 cm, the proposed method could detect protruding obstacles larger than 4 cm in height, as well as negative obstacles, with high accuracy.

In order to demonstrate the robustness of the proposed method, the conventional method[31] was applied to the indoor and outdoor data set for comparison with the proposed method. The conventional method used two Lidar sensors, which is tilted down toward the ground. In order to extract traversable terrains, the conventional method uses the cascade of filters that considers the height of each scan point and the neighboring points.

Fig. 13 shows a qualitative comparison between the conventional method and the proposed method for the outdoor dataset. Fig. 13(a) presents the classification results of traversable region by the conventional method. Compared with the hand labeled ground truth in Fig. 13(c), there are many points that were misclassified as obstacles in

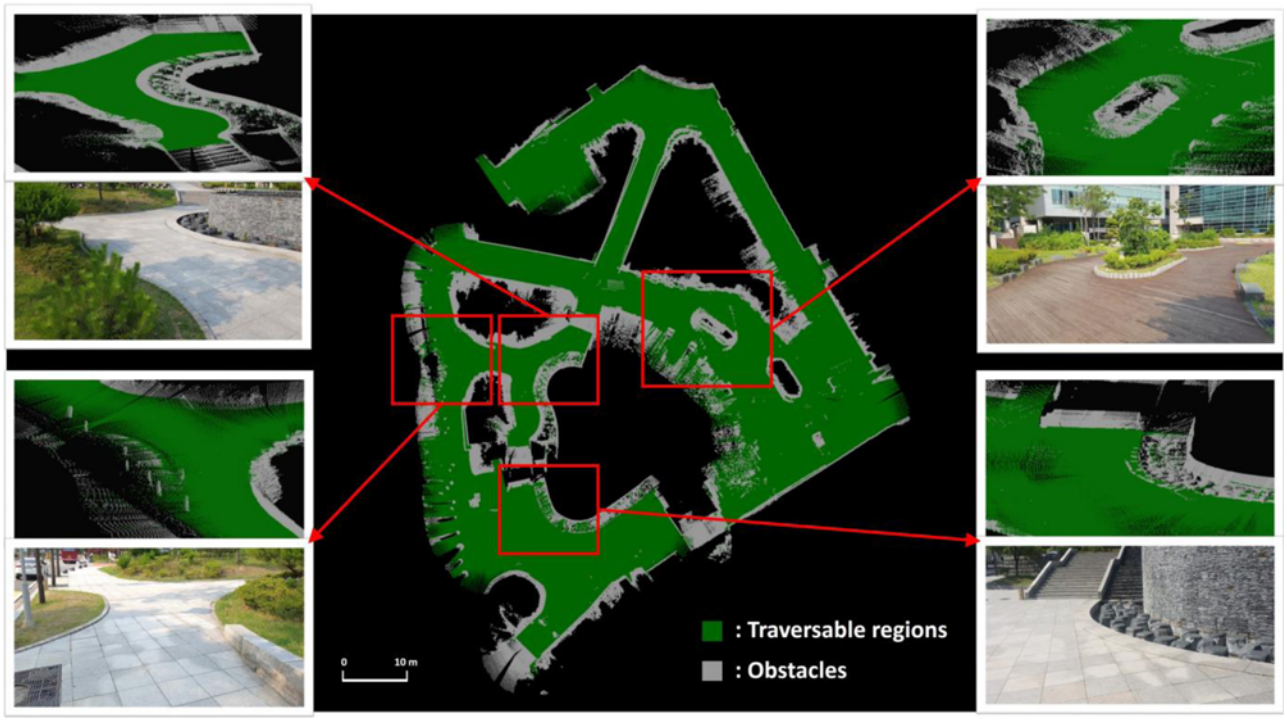

Fig. 12 Classification results in urban outdoor environments with magnified view of area of the test scene

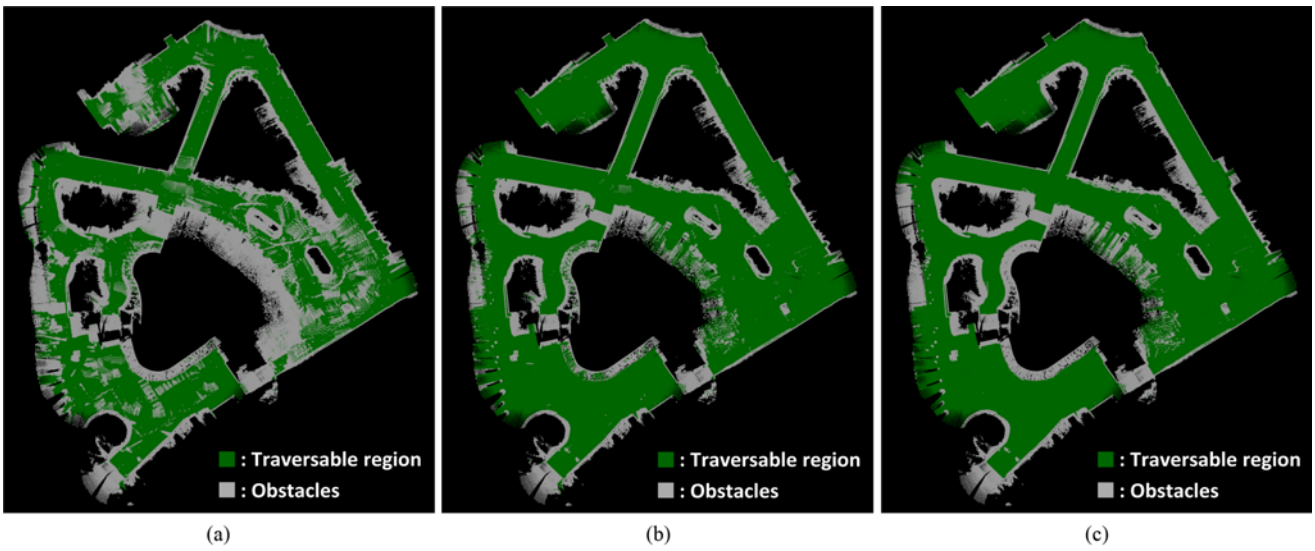

Fig. 13 Classification results for the outdoor data set., (a) the conventional method, (b) the proposed method, (c) hand-labeled ground truth

the middle of the traversable terrain. On the other hand, the classification result of the proposed method was similar to the ground truth, as shown in Fig. 13(b). The quantified evaluation for the classification results is shown in Table 2. For the indoor data set, the proposed method shows slightly better performance than the conventional method in terms of precision and specificity. On the other hand, the proposed method outperforms the conventional method for the outdoor data set. Especially, the specificity of the conventional method was 0.5183, which means that 48.17% of the obstacles were missing. Considering that specificity of the proposed method is 0.9378, most of these missing obstacle could be detected by our proposed method.

Table 2 Evaluation for the proposed and the conventional method

Data set	Method	Precision	Recall	Specificity
Indoor	proposed	0.9999	0.9963	0.9982
	conventional	0.9987	0.9975	0.9831
Outdoor	proposed	0.9903	0.9977	0.9378
	conventional	0.9200	0.8715	0.5183
Both	proposed	0.9917	0.9975	0.9424
	conventional	0.9321	0.8899	0.5541

5. Conclusion

In this paper, we suggest a method for terrain classification on the basis of a supervised learning approach. First, we proposed a method for calibrating the range bias error of 2D laser sensors to measure a terrain with high accuracy. By applying the bias calibration method, the terrain surface could be measured with high accuracy in a geometric manner.

We used a novel terrain feature that was calculated based on rolling windows, to complement the sparse data set of the 2D laser sensors with a single scan. Our approach for terrain classification used only positively labeled training data. The classification criteria were learned on the basis of SVDD, which is appropriate for this type of training data. With our approach, the classification criteria were easily obtained by steering a robot in target site, even when different sensors and robots were used.

In order to validate our approach, we operated the platforms that consists of different sensors and robots, on diverse terrain types. In the indoor experiment, the proposed method was able to detect protruding obstacles taller than 1 cm, as well as negative obstacles. The same techniques were applied to the outdoor experiment, with a different platform setup. With our approach, we were able to classify the terrain data into the traversable region and obstacles, with high accuracy. Consequently, the robustness of our algorithm was verified in experiments that were conducted under different operational conditions in the indoor and outdoor environments.

ACKNOWLEDGEMENT

This work was supported by the NRF, MSIP (NRF-2017R1A2A1 A17069329), also supported by the Agriculture, Food and Rural Affairs Research Center Support Program (714002-07), MAFRA, also supported by the Industrial Convergence Core Technology Development Program (No. 10063172) funded by MOTIE, Korea.

REFERENCES

1. Omron Corporation, “Mobile Robots,” https://industrial.omron.us/en/products/mobile-robots (Accessed 16 JUL 2018)
2. Amazon Robotics, “Amazon Robotics,” https://amazonrobotics.com/ (Accessed 24 JUL 2018)
3. ADAM, “Introducing the ADAM Solution,” http://www.adamrobot.com/en-ca/page/services (Accessed 24 JUL 2018)
4. Swisslog, “TransCar Automated Guided Vehicle,” https://www.swisslog.com/en-us/healthcare/products/material-transport/transcar-automated-guided-vehicle (Accessed 24 JUL 2018)
5. Savioke, http://www.savioke.com/hospitality-1 (Accessed 24 JUL 2018)
6. Kumar, S., Karthik, M. S., and Krishna, K. M., “Markov Random Field Based Small Obstacle Discovery over Images,” Proc. of IEEE International Conference on Robotics and Automation, pp. 494-500, 2014.
7. Vernaza, P., Taskar, B., and Lee, D. D., “Online, Self-Supervised Terrain Classification via Discriminatively Trained Submodular Markov Random Fields,” Proc. of IEEE International Conference on Robotics and Automation, pp. 2750-2757, 2008.
8. Kim, D., Sun, J., Oh, S. M., Rehg, J. M., and Bobick, A. F., “Traversability Classification Using Unsupervised On-Line Visual Learning for Outdoor Robot Navigation,” Proc. of IEEE International Conference on Robotics and Automation, pp. 518-525, 2006.
9. Howard, A., Turmon, M., Matthies, L., Tang, B., Angelova, A., and Mjolsness, E., “Towards Learned Traversability for Robot Navigation: From Underfoot to the Far Field,” Journal of Field Robotics, Vol. 23, Nos. 11-12, pp. 1005-1017, 2006.
10. Waymo, https://waymo.com/tech/ (Accessed 24 JUL 2018)
11. Andersen, J. C., Blas, M. R., Ravn, O., Andersen, N. A., and Blanke, M., “Traversable Terrain Classification for Outdoor Autonomous Robots Using Single 2D Laser Scans,” Integrated Computer-Aided Engineering, Vol. 13, No. 3, pp. 223-232, 2006.
12. Ye, C., “Navigating a Mobile Robot by a Traversability Field Histogram,” IEEE Transactions on Systems, Man, and Cybernetics, Part B (Cybernetics), Vol. 37, No. 2, pp. 361-372, 2007.
13. Ye, C. and Borenstein, J., “A Novel Filter for Terrain Mapping with Laser Rangefinders,” IEEE Transactions on Robotics, Vol. 20, No. 5, pp. 913-923, 2004.
14. Tanaka, Y., Ji, Y., Yamashita, A., and Asama, H., “Fuzzy Based Traversability Analysis for a Mobile Robot on Rough Terrain,” Proc. of IEEE International Conference on Robotics and Automation (ICRA), pp. 3965-3970, 2015.
15. McDaniel, M. W., Nishihata, T., Brooks, C. A., Salesses, P., and Iagnemma, K., “Terrain Classification and Identification of Tree Stems Using Ground-Based Lidar,” Journal of Field Robotics, Vol. 29, No. 6, pp. 891-910, 2012.
16. Larson, J. and Trivedi, M., “Lidar based Off-Road Negative Obstacle Detection and Analysis,” Proc. of 14th International IEEE Conference on Intelligent Transportation Systems (ITSC), pp. 192-197, 2011.
17. Wurm, K. M., Kümmerle, R., Stachniss, C., and Burgard, W., “Improving Robot Navigation in Structured Outdoor Environments by Identifying Vegetation from Laser Data,” Proc. of IEEE/RSJ International Conference on Intelligent Robots and Systems, pp. 1217-1222, 2009.
18. Wurm, K. M., Kretzschmar, H., Kümmerle, R., Stachniss, C., and Burgard, W., “Identifying Vegetation from Laser Data in Structured Outdoor Environments,” Robotics and Autonomous Systems, Vol. 62, No. 5, pp. 675-684, 2014.
19. Sinha, A. and Papadakis, P., “Mind the Gap: Detection and Traversability Analysis of Terrain Gaps Using Lidar for Safe Robot Navigation,” Robotica, Vol. 31, No. 7, pp. 1085-1101, 2013.

20. Heckman, N., Lalonde, J.-F., Vandapel, N., and Hebert, M., "Potential Negative Obstacle Detection by Occlusion Labeling," Proc. of IEEE/RSJ International Conference on Intelligent Robots and Systems, pp. 2168-2173, 2007.

21. Bellone, M., Messina, A., and Reina, G., "A New Approach for Terrain Analysis in Mobile Robot Applications," Proc. of IEEE International Conference on Mechatronics (ICM), pp. 225-230, 2013.

22. Suger, B., Steder, B., and Burgard, W., "Traversability Analysis for Mobile Robots in Outdoor Environments: A Semi-Supervised Learning Approach Based on 3D-Lidar Data," Proc. of IEEE International Conference on Robotics and Automation (ICRA), pp. 3941-3946, 2015.

23. Santamaria-Navarro, À., Teniente, E. H., Morta, M., and Andrade-Cetto, J., "Terrain Classification in Complex Three-Dimensional Outdoor Environments," Journal of Field Robotics, Vol. 32, No. 1, pp. 42-60, 2015.

24. Adams, M. D. and Probert, P. J., "The Interpretation of Phase and Intensity Data from AMCW Light Detection Sensors for Reliable Ranging," The International Journal of Robotics Research, Vol. 15, No. 5, pp. 441-458, 1996.

25. Ye, C. and Borenstein, J., "Characterization of a 2D Laser Scanner for Mobile Robot Obstacle Negotiation," Proc. of IEEE International Conference on Robotics and Automation, pp. 2512-2518, 2002.

26. Okubo, Y., Ye, C., and Borenstein, J., "Characterization of the Hokuyo URG-04LX Laser Rangefinder for Mobile Robot Obstacle Negotiation," Proc. of SPIE, Vol. 7332, 2009. (DOI: 10.1117/12.818332)

27. Borges, G. A. and Aldon, M.-J., "Line Extraction in 2D Range Images for Mobile Robotics," Journal of Intelligent and Robotic Systems, Vol. 40, No. 3, pp. 267-297, 2004.

28. Tax, D. M. and Duin, R. P., "Support Vector Domain Description," Pattern Recognition Letters, Vol. 20, Nos. 11-13, pp. 1191-1199, 1999.

29. Tax, D. M. and Duin, R. P., "Support Vector Data Description," Machine Learning, Vol. 54, No. 1, pp. 45-66, 2004.

30. Moon, C.-B., Chung, W., and Doh, N. L., "Observation Likelihood Model Design and Failure Recovery Scheme Toward Reliable Localization of Mobile Robots," International Journal of Advanced Robotic Systems, Vol. 7, No. 4, pp. 117-126, 2010.

31. Morales, Y., Carballo, A., Takeuchi, E., Aburadani, A., and Tsubouchi, T., "Autonomous Robot Navigation in Outdoor Cluttered Pedestrian Walkways," Journal of Field Robotics, Vol. 26, No. 8, pp. 609-635, 2009.